BATCH: jp8d19 USER: vkb69 DIV: @xyv04/data1/CLS_pj/GRP_jx/JOB_i33/DIV_jp063214x DATE: July 18, 2006

Early Excited State Dynamics of 6-Styryl-Substituted Pyrylium Salts Exhibiting Dual Fluorescence

Anatolio Pigliucci,[†] Peter Nikolov,[‡] Abdul Rehaman,[†] Laura Gagliardi,[†] Christopher J. Cramer,[§] and Eric Vauthey*,[†]

Department of Physical Chemistry, University of Geneva, 30 Quai Ernest-Ansermet, CH-1211 Geneva, Switzerland, Institute of Organic Chemistry with Center of Phytochemistry, Bulgarian Academy of Sciences, 1113 Sofia, Bulgaria, and Department of Chemistry and Supercomputing Institute, University of Minnesota, 207 Pleasant St. SE, Minneapolis, Minnesota 55455-0431

Received: May 25, 2006; In Final Form: June 20, 2006

A series of 6-styryl-2,4-diphenylpyrylium salts exhibiting dual fluorescence has been investigated by fluorescence up-conversion in conjunction with quantum chemical calculations. The short-wavelength emission is due to an excited state localized on the pyrylium fragment and the long-wavelength emission arises from a charge-transfer state delocalized over the whole molecule. The two fluorescing states do not exhibit a precursor−sater relationship. The rise time of the short-wavelength fluorescence is smaller than 200 fs, and that of the long-wavelength emission depends on the electron-donating property of the styryl group substituent. The rise is almost prompt with the weaker donors but is slower and wavelength and viscosity dependent with the strongest electron-donating group. A model involving a S_2/S_1 conical intersection is proposed to account for these observations.

Introduction

Pyrylium salts (PS) represent an important class of dyes that has found many applications such as laser and Q-switch dyes,[1−7] organic luminophores,[8] near-IR absorbing dyes,[9] pH-sensors,[10] and textile dyes.[11] They have also been used in various synthetic procedures.[12−15]

On the other hand, several PS are characterized by unusual photophysical properties that have been discussed in many reports. In general, 2,4,6-trisubstituted PS with three identical substituents, e.g., 2,4,6-triaryl PS, as well as some blocked PS are considered as two-dimensional chromophoric systems with X and Y absorption bands.[16−23] The photophysical and nonlinear properties of PS dimers that tend to be formed in low polarity solvents have been investigated in detail by Markovitsi and co-workers.[20,23−25] Kossanyi and co-workers have reported the observation of dual emission from blocked PS and explained it in terms of two excited states with different geometries.[26−28] The appearance of dual fluorescence has also been reported with other PS such as thiopyrylium salts and PS with biphenyl groups.[18,29] Some authors have also assigned the anomalous fluorescence to a twisted intramolecular charge-transfer (TICT) state.[18,26] In all these investigations wih systems exhibiting dual emission, the time resolution of the measurements was not high enough to monitor the buildup dynamics of the anomalous fluorescence. Despite this, a precursor−sater relationship between the two fluorescent states was assumed. Finally, it should be noted that the presence of a nonemissive TICT state has also been invoked to account for the viscosity-dependent fluorescence quantum yield a PS with an electron-donating group.[21] This hypothesis is further supported by a recent investigation using ultrafast transient absorption and fluorescence up-conversion.[30]

In a previous paper,[31] the unusual fluorescence properties of 6-styryl-2,4-disubstituted PS in solvents of different polarities have been reported. Their UV−vis absorption spectra are characterized by two well-separated bands. The high energy band with a maximum in the 340−400 nm spectral region is apparently strongly localized on the pyrylium fragment of the molecule and has been assigned to the S_0-S_2 transition. The low energy band, with a maximum in the 420−530 nm region, depending on the nature of the substituent in the 6-position of the pyrylium fragment, corresponds to the S_0-S_1 transition. Excitation of the S_0-S_2 transition gives rise to two distinct fluorescence bands, one that is located between the S_0-S_2 and the S_0-S_1 absorption bands and the other that is a mirror image of the S_0-S_1 absorption band. The analysis of the experimental data indicates that the low energy emission is the ordinary S_1-S_0 fluorescence associated with the whole conjugated system of the PS. On the other hand, the short-wavelength emission, located at an energy higher than that for the S_0-S_1 absorption band has been ascribed to a local fluorescence related to the pyrylium fragment of the molecule. Consequently, the high and low energy emission bands have been designated as L and D bands, for localized and delocalized, respectively.[31]

In nonprotic solvents, the decay of the L fluorescence was found to be monoexponential with a lifetime varying between 1.5 and 2 ns. On the other hand, the decay of the D fluorescence could not be reproduced with less than three exponential functions, with about 90% of the total amplitude associated with a 3.5−4 ns lifetime. However, no precursor−sater relationship between both emissions could be evidenced. In fact, no rising component of the D-fluorescence could be detected, the time resolution of the measurements being of the order of 300 ps.

We report here on an investigation of the early fluorescence dynamics of several 6-styryl-2,4-diphenyl PS (see Figure 1) using femtosecond fluorescence up-conversion to elucidate the conversion mechanism between the two emitting states. These

* Corresponding author. E-mail: eric.vauthey@chiphy.unige.ch.
[†] University of Geneva.
[‡] Bulgarian Academy of Sciences.
[§] University of Minnesota.

10.1021/jp063214x CCC: $33.50
Published on Web 00/00/0000 PAGE EST: 6.4

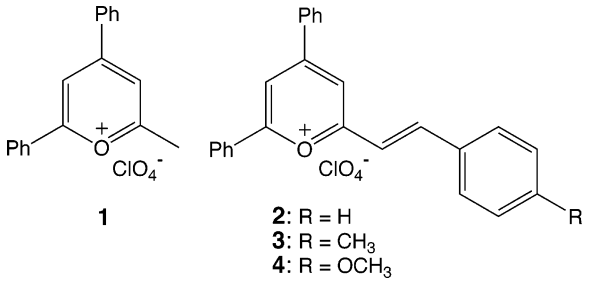

Figure 1. Structure of the PS investigated.

PS differ by the electron-donating properties of the substituent on the styryl group. Therefore, the extent of charge-transfer (CT) character of the D transition can be expected to increase from compounds **2**−**4**. For comparison, a PS dye with a methyl group instead of the styryl substituent (compound **1**) and exhibiting only the L fluorescence was investigated as well. To get a deeper insight into the electronic character of the lowest electronic states of these dyes, quantum chemistry calculations on compounds **2** and **4** have also been performed. A possible model accounting for the "non-Kasha" fluorescence behavior of these dyes, which is also based on these calculations, will then be proposed.

Experimental Section

Apparatus. The fluorescence up-conversion setup has already been described in detail elsewhere.[32] In brief, the frequency doubled output of a Kerr lens mode-locked Ti:Sapphire laser (Tsunami, Spectra-Physics) was used for excitation of the samples at 400 nm. This excitation wavelength was used for all measurements. The output pulses centered at 800 nm had a duration of about 100 fs and a repetition rate of 82 MHz. The pump intensity on the sample was around 10^{14} photons·cm^{-2}·pulse^{-1}. The polarization of the pump pulses was at a magic angle relative to that of the gate pulses. Experiments were carried out in a 0.4 mm thick rotating cell. The absorbance of the samples at 400 was around 0.1. The full width at half-maximum (fwhm) of the instrument response function was ca. 210 fs.

Samples. The synthesis of the pyrylium perchlorate salts **1**−**4** has been described in the literature.[31] These compounds have been purified by repeated recrystallization and the amount of impurity has been estimated to be less than 1%. The solvents, dichloromethane (DCM), ethanol (EtOH) and butanol (BuOH) were of the highest commercially available purity and were used as received. All solutions were purged with argon before measurements. A substantial degradation of the sample solutions was observed after prolonged irradiation. Such a poor photostability of many PS dyes in solution is well-known,[33] and therefore fresh samples were used for each measurement. To ensure that this degradation had no effect on the fluorescence up-conversion data, the time profiles obtained by scanning the time delay in both forward and backward directions were compared. Unless specified, all measurements have been performed at 20 ± 2 °C.

Computational Methods. The ground-state singlet gas-phase geometries of **2** and **4** were fully optimized at the density functional level of theory (DFT) using the BP86 and B3LYP functionals[34,35] and a [3s2p1d] basis set.[36] Electronic vertical excitation energies and oscillator strengths were then computed using time-dependent density functional theory[37] (TDDFT) and configuration interaction over single excitations[38] (CIS). For the TDDFT calculations, both the pure BP86 and hybrid B3LYP[34,39−41] functionals were examined in conjunction with the [3s2p1d] basis set; for the CIS calculations, the INDO/S2 Hamiltonian[42,43] was used. In addition, the gas-phase geometries of the first and second singlet excited states of **4** were optimized at the TDB3LYP/[3s2p1d] level. Solvatochromic effects were computed at the VEM4.2 level of theory based on the CIS/INDO/S2 results. TDDFT calculations were carried out using Turbomole version 5.8.0,[44,45] and CIS calculations were carried out using ZINDO-MN version 1.2.[46]

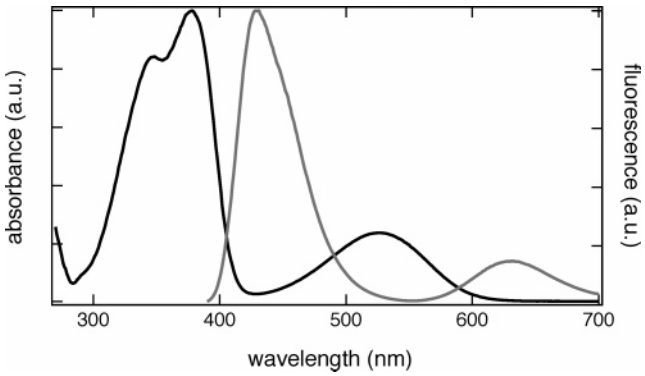

Figure 2. Absorption (black) and fluorescence spectra (gray, excitation at 360 nm) of **4** in DCM.

TABLE 1: L and D Absorption and Emission Maxima (Excitation at 360 nm) of 1−4 in Various Solvents

		1	**2**		**3**		**4**	
		L	L	D	L	D	L	D
DCM	λ_{max}^{abs} (nm)	383	383	470	383	487	383	529
	λ_{max}^{em} (nm)	430	430	540	430	570	430	630
EtOH	λ_{max}^{abs} (nm)	373	373	450	373	450	373	507
	λ_{max}^{em} (nm)	440	440	555	440	570	440	645
BuOH	λ_{max}^{abs} (nm)	373					373	516
	λ_{max}^{em} (nm)	430					430	636

Results

Early Fluorescence Dynamics. The absorption and fluorescence spectra of the dyes **1**−**4** have been discussed in detail in ref 31, and the band maxima are listed in Table 1. As an example, the spectra of **4** are shown in Figure 2. Both the absorption and fluorescence spectra of the other dyes in the L band region are very similar. On the other hand, the D band shifts to shorter wavelength by going from **4** to **2**. For the latter compound, the D band overlaps substantially with the L band, whereas it is absent with **1**, where the styryl group is replaced by a methyl group.

The areas of both L and D absorption bands of **4** in DCM are independent of temperature between −5 and +25 °C. The same behavior was observed with the D fluorescence band of the same dye. On the other hand, a 5% decrease of the area of its L emission band was found by going from −5 to +25 °C. The same small decrease was measured with **1**. Although the L fluorescence maximum remains constant in the temperature range investigated, the D fluorescence band exhibits a hypsochromic shift of about 3 cm^{-1}·K^{-1} with increasing temperature.

Figure 3 shows time profiles of the early fluorescence of **1** and **2** in DCM. The rise of all these profiles is essentially prompt; i.e., its time constant is shorter or equal to the fwhm of the instrument response function. After this rise, the L fluorescence at 430 nm of both **1** and **2** exhibits a weak decaying component with a time constant of the order of 1.5−2 ps (see Table 2). At the other wavelengths investigated, the fluorescence intensity remains constant within the time window of the measurement (10 ps).

In EtOH, the early dynamics of the L fluorescence of **1** and **2** is qualitatively the same as in DCM. On the other hand, the

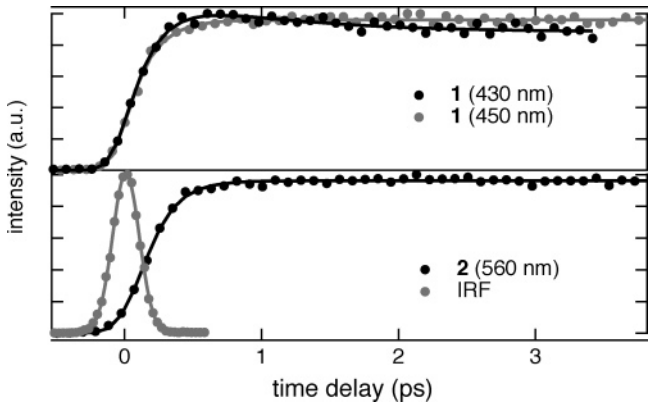

Figure 3. Time profiles of the L fluorescence of **1** (top) and of the D fluorescence of **2** (bottom) in DCM. The instrument response function (IRF) is shown for comparison.

TABLE 2: Parameters Obtained from the Fit of a Biexponential Function to the Time Profiles of the Early Fluorescence of 1−4 in DCM upon 400 nm Excitation[a]

dye	λ (nm)	band	A_1	τ_1 (ps)	A_2	τ_2 (ps)
1	430	L	−1	0.16	0.19	1.5
	450	L	−1	0.17	0	
2	430	L	−1	0.14	0.14	2.1
	450	L	−1	0.19	0	
	560	D	−1	0.20	0	
	610	D	−1	0.20	0	
3	430	L	−1	0.13	0.18	1.8
	450	L	−1	0.15	0	
	560	D	−0.90	0.24	−0.10	2.3
	580	D	−0.85	0.23	−0.15	2.3
4	430	L	−1	0.15	0	
	450	L	−1	0.20	0	
	480	L	−0.86	0.19	−0.14	1.7
	600	D	−1	0.18	0.2	1.8
	630	D	−1	0.30	0.1	1.8
	650	D	−1	0.36	0	

[a] Only the components with a time constant shorter than 10 ps are listed.

TABLE 3: Parameters Obtained from the Fit of a Biexponential Function to the Time Profiles of the Early Fluorescence of 1−4 in EtOH upon 400 nm Excitation[a]

dye	λ (nm)	band	A_1	τ_1 (ps)	A_2	τ_2 (ps)
1	430	L	−1	0.16	0.15	1.4
2	430	L	−1	0.17	0.20	1.5
	450	L	−1	0.19	0	
	500	L/D	−0.91	0.25	−0.09	2.0
	540	D	−0.70	0.22	−0.30	1.6
3	450	L	−1	0.11	0	
	550	D	−0.72	0.20	−0.28	1.5
	580	D	−0.86	0.23	−0.14	1.6
4	450	L	−1	0.20	0	
	600	D	−1	0.30	0	
	620	D	−1	0.36	0	
	640	D	−1	0.59	0	

[a] Only the components with a time constant shorter than 10 ps are listed.

rise of the D fluorescence of **2** was found to be biphasic, with a prompt and a ~1.5 ps component. The amplitude of this slower component apparently increases with increasing wavelength. However, it should be noted that at 500 nm, both L and D emissions contribute to the signal. All the parameters obtained upon analysis of these time profiles are listed in Tables 2 and 3.

The early L fluorescence dynamics of **3** in both DCM and EtOH is essentially the same as that of **1** and **2**. The rise of its

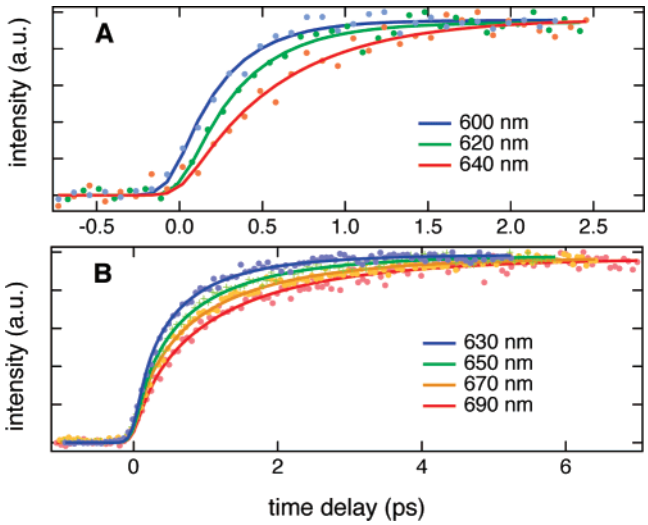

Figure 4. Time profiles of the D fluorescence of **4** in EtOH (**A**) and BuOH (**B**).

D-fluorescence is also biphasic with a 1.5−2.3 ps component in both solvents. Because of the small amplitude of this slower component, the uncertainty on its time constant is relatively large.

As for the other dyes, the rise of the L fluorescence of **4** is essentially prompt. On the other hand, the early dynamics of the D fluorescence in both solvents differs substantially from that of **2** and **3**. Indeed, it is not prompt and it exhibits a marked wavelength dependence. In DCM, the rise time increases from 180 to 360 fs by going from 600 to 650 nm. In EtOH, the rise of the D fluorescence is substantially slower and increases with wavelength as well, as shown in Figure 4A. To test whether the slower rise in EtOH is related to the higher viscosity of this solvent compared with DCM (η(DCM) = 0.44 cP, η(EtOH) = 1.2 cP at 20 °C),[47] the early fluorescence dynamics of **4** was also investigated in a more viscous solvent, namely BuOH (η(BuOH) = 3.3 cP at 20°).[47] As shown in Figure 4B, the rise of the fluorescence intensity is clearly slower than that in the other solvents and the wavelength dependence is still present. This rise could not be very well reproduced with a monoexponential function, especially above 650 nm and thus a biexponential function had to be used. The resulting best-fit parameters are listed in Table 3. The average rise times are also listed to enable comparison with the other solvents. Interestingly, a plot of the rise time measured as the longest wavelength as a function of solvent viscosity is almost perfectly linear with a slope of 0.3 ps/cP. Although the number of investigated solvents is small, this correlation is probably not coincidental.

Quantum Chemistry Calculations. To understand in more detail the electronic character of the various excited singlet states of these compounds, TDDFT calculations were carried out for gas-phase molecular geometries optimized using the BP86 and B3LYP functionals. In addition, CIS calculations at the INDO/S2 level of theory were also performed. Both levels of theory agree that the frontier orbitals of the styrylpyrylium system, illustrated in Figure 5 for **4**, are characterized as HOMO−1, a π orbital formed as a combination of π orbitals on both of the unsubstituted phenyl rings attached to the pyrylium heterocycle; HOMO, a π orbital on the aromatic ring and olefin of the styryl fragment; and LUMO and LUMO+1, π orbitals almost entirely localized on the pyrylium ring.

Both levels of theory are also in good agreement as to the nature of the excitations. The S_1 state is well described as a one-electron intramolecular CT state deriving from a HOMO

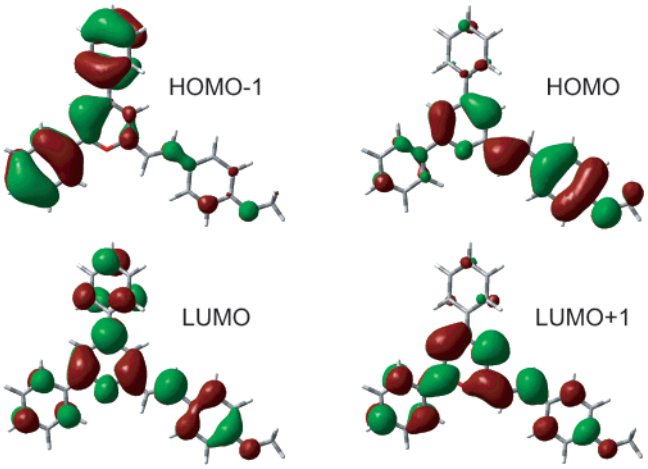

Figure 5. Frontier molecular orbitals (HOMO−1, HOMO, LUMO, and LUMO+1) for **4** computed at the B3LYP/[3s2p1d] level of theory. Orbital contours are drawn at the 0.03 au level.

TABLE 4: Parameters Obtained from the Fit of a Biexponential Function to the Time Profiles of the Early Fluorescence of 4 in BuOH upon 400 nm Excitation[a]

λ (nm)	band	A_1	τ_1 (ps)	A_2	τ_2 (ps)	$\langle\tau\rangle^b$ (ps)
450	L	−1	0.19	0		
630	D	−0.66	0.39	−0.34	1.0	0.60
650	D	−0.60	0.42	−0.40	1.43	0.82
670	D	−0.60	0.46	−0.40	1.9	1.03
690	D	−0.55	0.47	−0.45	2.1	1.20

[a] Only the components with a time constant shorter than 10 ps are listed. [b] Calculated as $\langle\tau\rangle = -A_1\tau_1 - A_2\tau_2$.

TABLE 5: Excitation Energies, *E* (eV), Wavelengths, λ (nm), and Oscillator Strengths, *f* (au), for Vertical Excitations in 2 and 4 at Various Levels of Theory

	CIS/INDO/S2			TDBP86			TDB3LYP		
transition	*E*	λ	*f*	*E*	λ	*f*	*E*	λ	*f*
				2					
$S_0 \rightarrow S_1$	3.02	410 [401][a]	1.11	2.35	527	0.42	2.70	460	0.68
$S_0 \rightarrow S_2$	3.80	326 [316]	0.98	2.49	497	0.02	3.14	395	0.01
$S_0 \rightarrow S_3$	4.15	299 [291]	0.02	2.65	468	0.01	3.21	386	0.26
				4					
$S_0 \rightarrow S_1$	2.75	451 [432]	1.33	2.06	601	0.38	2.45	506	0.73
$S_0 \rightarrow S_2$	3.77	329 [316]	0.60	2.66	466	0.37	3.15	393	0.31
$S_0 \rightarrow S_3$	4.00	310 [301]	0.37	2.74	453	0.01	3.32	373	0.56

[a] Excitation wavelengths in brackets in this column refer to VEM4.2 predictions in alcohol solution.

to LUMO excitation. The S_2 and S_3 states are best described as alternative linear combinations of one-electron excitations from HOMO to LUMO+1 and HOMO−1 to LUMO. As such, they involve substantially less charge transfer from the styryl fragment to the pyrylium. The energies of these excitations at the various levels of theory are presented in Table 5.

Excitation energies at the TD B3LYP level are in fairly good agreement with experiment. At the TD BP86 and CIS/INDO/S2 level, the qualitative ordering of the states remains the same, but the predicted energetics are substantially to the red and to the blue of experiment, respectively. These results are quite consistent with the known tendencies of (i) TDDFT to underestimate the energy separation between ground states and CT excited states (particularly for pure density functionals such as BP86) and (ii) CIS/INDO/S2 to overestimate the transition energies associated with CT excited states and delocalized π excitations.[48] However, the CIS/INDO/S2 results are useful insofar as they permit an analysis of solvatochromic effects in

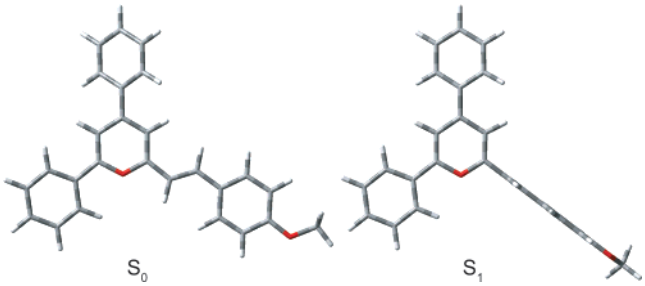

Figure 6. Optimized geometries for the S_0 and S_1 states of **4** at the (TD)B3LYP/[3s2p1d] level of theory.

alcohol at the VEM4.2 level. In general, the effects are predicted to be relatively small: a 10−20 nm blue shift is predicted for the first three excitations. If these solvatochromic shifts are added to the gas-phase B3LYP predictions, the agreement with experiment remains good.

According to these calculations, both S_0-S_2 and S_0-S_3 transitions contribute to the broad absorption band between 300 and 400 nm. This explains why the L fluorescence band is not really its mirror image. Indeed, the L fluorescence band is much narrower (fwhm ∼3000 vs ∼6350 cm^{-1}), and the pronounced shoulder around 345 nm has no equivalent in the fluorescence spectrum.

When the geometries of the first two excited states of **4** are optimized, the lower energy state twists about the styryl moiety and minimizes to a classic TICT structure (Figure 6). Vertical emission from this state is predicted to occur at approximately 1200 nm at the TD B3LYP level, which is substantially to the red of experiment. However, this large red shift is consistent with the known tendency mentioned above of TDDFT to underestimate the energy of CT excited states. Because, with the twisted geometry, CT is effectively complete, it is not surprising that this inaccuracy arises even for the hybrid B3LYP functional. The S_2 state, on the other hand, remains planar after relaxation. The major difference between S_0 and S_2 equilibrium geometries is the twist angle of the phenyl group in the 4 position, which changes from 8° in S_0 to 1° in S_2. Vertical emission from this state is predicted to occur at about 430 nm, which is in good agreement with experiment.

Discussion

Molecules exhibiting dual fluorescence are relatively scarce, in agreement with Kasha's rule. Most observations of dual emission are due to molecules experiencing a chemical process, such as electron or proton transfer,[49−53] or a substantial conformational change on the excited-state surface.[54,55] It should be noted that in these cases, the excited state responsible for the low energy fluorescence cannot be directly populated upon optical excitation. These cases cannot really be considered as exceptions of Kasha's rule as the fluorescence always occurs from the lowest singlet excited state. The situation is different for the PS dyes investigated here, because their absorption spectra exhibit both L and D bands and therefore the low energy fluorescence can be generated upon direct excitation in the D band. Therefore, L and D emissions can be considered as S_2-S_0 and S_1-S_0 emissions, respectively. Zn−tetraphenylporphine (ZnTPP) is most probably the best known molecule, which exhibits fluorescence from both S_2 and S_1 states.[56] Time-resolved measurements have shown that these emissions have a precursor−sater relationship, indicating the population of the S_1 state upon internal conversion from S_2.[56]

The striking feature of the styrylpyrylium dyes **2**−**4** compared to ZnTPP is the absence of precursor−sater relationship between

the S_2 (L) and S_1 (D) emission profiles. Indeed, the rise time of the D fluorescence of **2**−**4** is much faster than the decay time of the L fluorescence.

Before proposing a model that could account for this observation, we will discuss the origin of the slower rising or decaying components, τ_2, observed in both L and D emission in DCM and EtOH. According to Tables 2 and 3, τ_2 amounts to about 2 ps independently of the PS dye, the solvent and the emission wavelength. Its amplitude, A_2, is wavelength dependent: when different from zero, it is positive on the blue side of the L fluorescence band, indicating a decay and negative at longer wavelength (see **4** in DCM). Moreover, its magnitude tends to increase with wavelength (see **2** in EtOH). These two observations suggest that this component is not related to population dynamics. If it were the case, A_2 should always be positive in the L band and negative in the D band, as expected for a transfer of population from the L to the D states. Moreover, the observation of this component with compound **1** clearly indicates a different origin. The wavelength dependence of A_2 rather suggests a temporal evolution of the shape of the fluorescence spectrum. Considering the value of τ_2, two processes can be envisaged: solvent relaxation and vibrational cooling.[57,58] According to dynamic Stokes shift measurements performed with coumarin 153, the solvation dynamics of DCM is biphasic with an ultrafast inertial component (100 fs and 50% relative amplitude) and a slower diffusive component of 1 ps.[59] For EtOH, three time constants have been reported: 390 fs (25%), 5ps (20%), and 30 ps.[59] These values do not agree very well with those of τ_2 found here. Therefore, dynamic Stokes shift seems not to be the main origin of this component. Vibrational cooling is known to lead to a narrowing of the fluorescence spectrum. This process appears as a decaying component on the edges of the fluorescence band and as a rise in the central region. Vibrational cooling takes place on different time scales, going from less than a picosecond to a few tens of picoseconds, depending apparently on the amount of vibrational excess energy.[58,60−64] The small time constant measured here is in agreement with a small excess excitation energy. The solvent dependence of this process is still not totally understood, although the slower cooling component has been reported to depend on the thermal diffusivity of the environment.[61] A joint contribution of both solvation and vibrational cooling dynamics to this component cannot be excluded.

The absence of a D band with **1** and the dependence of the D band maximum on the electron-donating properties of the styryl substituent indicate a CT character of this transition. This is fully supported by the calculations, which can very well reproduce the change of the absorption maximum of the D band by going from **2** to **4**. TDB3LYP and CIS/INDO/S2 both agree that the S_0−S_1 transition for **2** is blue shifted by about 40 nm relative to that for **4**, whereas the other two excitations are less sensitive to this substitution (as expected, because the S_0−S_2 and S_0−S_3 transitions are substantially more localized on the pyrylium fragment that is common to both **2** and **4**).

Moreover, triphenylpyrylium salts are well-known as electron-transfer photosensitizers,[15] and are characterized by a relatively low reduction potential. Kossanyi and co-workers[65] have reported the observation of CT absorption and fluorescence with donor−acceptor complexes composed of aromatic hydrocarbons as electron donors and of **1** as electron acceptor. The shape of these CT bands is very similar to those of the D bands measured here with **2**−**4**. Moreover, local excitation of **1** was found to be followed by both local and CT emissions as observed here for **2**−**4**.[65] Therefore, the D band can be unambiguously assigned to a CT transition. As the relative intensities of L and D bands of **2**−**4** are independent of the dye concentration, the formation of intermolecular donor−acceptor complexes can be safely excluded. Moreover, the absence of a temperature effect on the absorption spectrum of **4** also rules out the existence of an equilibrium between several conformations in the ground state.

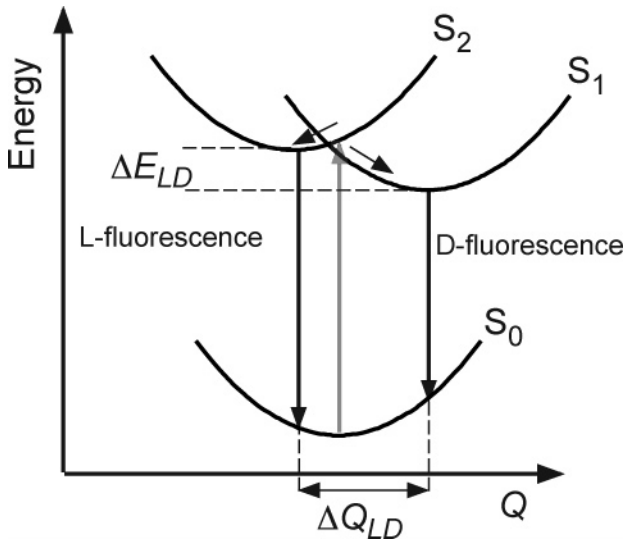

Figure 7. Hypothetical arrangement of the potential-energy surfaces of the lowest singlet excited states accounting for the observed early L and D fluorescence dynamics of **2**−**4**.

The fact that both L and D emissions exhibit an almost prompt rise and a distinct decay in the nanosecond time scale could be explained with an arrangement of potential-energy surfaces as shown in Figure 7. For the sake of simplicity, harmonic potentials have been assumed, but of course, their actual shape may differ substantially depending on the nature of the coordinate *Q*. Excitation in the L band prepares the excited state population away from equilibrium. Upon relaxation, a fraction of this population remains on the L potential, whereas the other crosses to the D potential. After thermalization, both populations are irreversibly "trapped" at the bottom of their potential and thus the two relaxed states are decoupled. In a multidimensional picture, the intersection region shown in Figure 7 corresponds to a conical intersection.[66,67] This picture is partially supported by TDDFT geometry optimization of the first two excited states of **4**. However, according to these calculations, the D state remains below the L state even after relaxation of the latter's geometry, and D emission at this geometry is predicted to occur at 510 nm. This result contradicts the above conical intersection hypothesis. However, the CT nature of S_1 causes its potential-energy surface to be predicted to be anomalously low at the TDDFT level. It is thus entirely possible that with more accurate energetics, a conical intersection between the S_1(D) and S_2(L) states might occur sufficiently near the ground-state geometry such that relaxation along the formally S_2 surface would result in a minimum that, at its own geometry, corresponds to a formally S_1 state from which L fluorescence can occur. Unfortunately, the levels of theory that would be required to offer more quantitative support than TDDFT for this phenomenon are not yet computationally practical for polyaromatic systems of this size.

As the transition from the L to D state can be considered as an intramolecular CT process, the coordinate *Q* should involve both solvent and intramolecular modes as it is generally the case for electron-transfer processes.[68] The TDDFT calculations point out the twisting motion of the styryl group as an important

coordinate. The occurrence of such a large amplitude motion can explain the viscosity dependence of the D fluorescence rise time measured with **4**. The wavelength-dependent rise of the D fluorescence found with this dye could be explained by a conical intersection located far from the D equilibrium state. Therefore, long-wavelength D emission appears only after relaxation of the D state population. On the other hand, the location of the conical intersection close to the equilibrium geometry of the L state is supported by the prompt rise of the L emission. It is, however, not absolutely clear whether the substantial structural change predicted for the CT state can be completed within a picosecond or less. The actual twist angle of the styryl group might be not as pronounced as that calculated. Here again it appears that a more definitive answer calls for higher level of theory. This is, however, a difficult problem even for smaller molecules such as the well-known 4-(dimethylamino)benzonitrile.[69]

Solvent modes could also contribute to the viscosity dependence of the D fluorescence rise measured with **4**. The average solvation times of DCM, EtOH and BuOH amount to 0.56, 16 and 63 ps, respectively, and are thus much larger than the fluorescence rise time. However, solvation dynamics is well-known to be multiphasic and even viscous solvents have an ultrafast component in their response. A much better agreement with the experiment is obtained if the initial solvation times of DCM, EtOH and BuOH, which have been reported to amount to 0.25, 0.29−1.4, and 1.45 ps,[59] respectively, are considered.

The differences in buildup dynamics of the D fluorescence observed with **2**−**4** might be explained by differences in the relative position of the excited-state potentials. In particular, the energy gap between the L and D states, ΔE_{LD}, increases by going from **2** to **4** as the electron-donating ability of the styryl substituent becomes larger. Similarly, the difference of equilibrium position along the coordinate, ΔQ_{LD}, can also be predicted to increase with the extent of CT character of the D state, especially if solvent modes are involved.

Both ΔE_{LD} and ΔQ_{LD} are the largest with **4**, and therefore a slower and wavelength-dependent rise time can be observed. On the other hand, the close to prompt D fluorescence rise of PS **2** and **3** can be explained by a smaller ΔQ_{LD} and hence by a conical intersection located closer to the equilibrium position of the D state.

The absence of a temperature dependence of the D fluorescence band measured with **4** shows that the D state is not thermally accessible from the L state and reciprocally, in agreement with this model. The small temperature effect observed with the L fluorescence of both **4** and **1** indicates that it is not related to the D state. The slightly larger L fluorescence quantum yield at lower temperature is most probably connected to a nonradiative deactivation pathway with a small temperature dependence.

Concluding Remarks

We have reported the first investigation of the anomalous fluorescence of PS dyes using ultrafast spectroscopy. The data show clearly the absence of a precursor−sater relationship between the two emitting states. These styrylpyrilium dyes thus exhibit exceptional photophysical properties. In this case, the violation of Kasha's rule is due to the fact that both thermally equilibrated states are totally uncoupled. The presence of a conical intersection seems to be the most plausible explanation for the quasi-prompt rise of the fluorescence from both states. This hypothesis partially supported by TDDFT calculations. However, higher level calculations, which are presently not computationally practical, would be required to obtain a deeper insight into the unusual photophysics of these dyes. Moreover, it would be interesting to perform similar measurements with other PS, which also exhibit dual fluorescence, to find out whether the unusual behavior observed here is a general feature of PS.

Acknowledgment. We thank Dr. Stefan Metzov from the Chemical Faculty of the University of Sofia for kindly supplying the pyrylium salts. This work was supported by the Fonds National Suisse de la Recherche Scientifique through the projects 200020-107466, 111072 (SCOPES) and 200021-111645, and by the U.S. National Science Foundation (CHE-0203346).

References and Notes

(1) Fakis, M.; Polyzos, J.; Tsigaridas, G.; Parthenios, J.; Fragos, A.; Giannetas, V.; Persephonis, P.; Mikroyannidis, J. *Chem. Phys. Lett.* **2000**, *323*, 111.
(2) Kotowski, T.; Skubiszak, W.; Soroka, J. A.; Soroka, K. B.; Stacewicz, T. *J. Lumin.* **1991**, *50*, 39.
(3) Luo, W.; Zhu, Z.; Yao, Y.; Ye, L.; Yuan, X. *Laser Chem.* **1990**, *10*, 259.
(4) Tripathi, S.; Wintgens, V.; Valat, P.; Toscano, V.; Kossanyi, J.; Bos, F. *J. Lumin.* **1987**, *37*, 149.
(5) Basting, D.; Schaefer, F.; Steyer, B. *Appl. Phys.* **1974**, *3*, 81.
(6) Rullière, C.; Declemy, A.; Balaban, A. T. *Can. J. Phys.* **1985**, *63*, 191.
(7) Williams, J. L. R.; Reynolds, G. A. *J. Appl. Phys.* **1968**, *39*, 5327.
(8) Yamamoto, N.; Okamoto, T.; Kawaguchi, M. *Nucl. Acids Symp. Ser.* **1993**, *29*, 83.
(9) Nakazumi, H.; Watanabe, S.; Kado, S.; Kitao, T. *Chem. Lett.* **1989**, 1039.
(10) Czerney, P.; Grummt, U.-W. *J. Chem. Res., Synopses* **1996**, 173.
(11) Simov, D.; Metsov, S.; Prangova, L. *Izvest. Khim.* **1986**, *19*, 428.
(12) *Pyrylium Salts: Syntheses, Reactions and Physical Properties*; Katritzky, A. R., Ed.; Academic Press: New York, 1982; Vol. suppl. 2.
(13) Ning, G.; Li, X. C.; Munakata, M.; Gong, W. T.; Maewake, M.; Kamiwaka, T. *J. Org. Chem.* **2004**, *69*, 1432.
(14) Gong, W.-T.; Li, X.-C.; Ning, G.-L.; Lin, Y. *J. Chem. Res.* **2004**, 444.
(15) Miranda, M. A.; Garcia, H. *Chem. Rev.* **1994**, *94*, 1063.
(16) Tripathi, S.; Simalty, M.; Kossanyi, J. *Tetrahedron Lett.* **1985**, *26*, 1995.
(17) Balaban, A. T.; Sahini, V.; Keplinger, E. *Tetrahedron* **1960**, *9*, 163.
(18) Parret, S.; Morlet-Savary, F.; Fouassier, J. P.; Inomata, K.; Matsumoto, T.; Heisel, F. *Bull. Chem. Soc. Jpn.* **1995**, *68*, 2791.
(19) Haucke, G.; Czerney, P.; Cebulla, F. *Ber. Bunsen-Ges. Phys. Chem.* **1992**, *96*, 880.
(20) Markovitsi, D.; Sigal, H.; Ecoffet, C.; Millie, P.; Charra, F.; Fiorini, C.; Nunzi, J. M.; Strzelecka, H.; Veber, M.; Jallabert, C. *Chem. Phys.* **1994**, *182*, 69.
(21) Lampre, I.; Marguet, S.; Markovitsi, D.; Delysse, S.; Nunzi, J. M. *Chem. Phys. Lett.* **1997**, *272*, 496.
(22) Tripathi, S.; Simalty, M.; Pouliquen, J.; Kossanyi, J. *Bull. Soc. Chim. Fr.* **1986**, 600.
(23) Lampre, I.; Markovitsi, D.; Fiorini, C.; Charra, F.; Veber, M. *J. Phys. Chem.* **1996**, *100*, 10701.
(24) Lampre, I.; Markovitsi, D.; Birlirakis, N.; Veber, M. *Chem. Phys.* **1996**, *202*, 107.
(25) Lampre, I.; Markovitsi, D.; Millie, P. *J. Phys. Chem.* **1997**, *101*, 90.
(26) Wintgens, V.; Pouliquen, J.; Kossanyi, J.; Williams, J. L. R.; Doty, J. C. *Polym. Photochem.* **1985**, *6*, 1.
(27) Lahmadi, F.; Valat, P.; Simalty, M.; Kossanyi, J. *Res. Chem. Intermed.* **1995**, *21*, 807.
(28) Lahmadi, F.; Valat, P.; Kossanyi, J. *New J. Chem.* **1995**, *19*, 965.
(29) Vollmer, F.; Rettig, W.; Birckner, E.; Haucke, G.; Czerney, P. *J. Inf. Rec. Mater.* **1994**, *21*, 497.
(30) Gulbinas, V.; Markovitsi, D.; Gustavsson, T.; Karpicz, R.; Veber, M. *J. Phys. Chem. A* **2000**, *104*, 5181.
(31) Nikolov, P.; Metzov, S. *J. Photochem. Photobiol. A* **2000**, *135*, 13.
(32) Morandeira, A.; Engeli, L.; Vauthey, E. *J. Phys. Chem. A* **2002**, *106*, 4833.
(33) Gazeau, M.-C.; Valat, P.; Wintgens, V.; Kossanyi, J. *J. Chem. Soc., Faraday Trans.* **1996**, *92*, 3051.
(34) Becke, A. D. *Phys. Rev. A* **1988**, *38*, 3098.

(35) Perdew, J. P. *Phys. Rev. B* **1986**, *33*, 8822.
(36) Schäfer, A.; Horn, H.; Ahlrichs, R. *J. Chem. Phys.* **1992**, *97*, 2571.
(37) Bauernschmitt, R.; Ahlrichs, R. *Chem. Phys. Lett.* **1996**, *256*, 454.
(38) Foresman, J. B.; Head-Gordon, M.; Pople, J. A.; Frisch, M. J. *J. Phys. Chem.* **1992**, *96*, 6.
(39) Lee, C.; Yang, W.; Parr, R. G. *Phys. Rev. B* **1988**, *37*, 785.
(40) Becke, A. D. *Chem. Phys.* **1993**, *98*, 5648.
(41) Stephens, P. J.; Devlin, F. J.; Chabalowski, C. F.; Frisch, M. J. *J. Phys. Chem.* **1994**, *98*, 11623.
(42) Ridley, J. E.; Zerner, M. C. *Theor. Chim. Acta* **1973**, *32*, 111.
(43) Li, J.; Williams, B.; Cramer, C. J.; Truhlar, D. G. *J. Chem. Phys.* **1999**, *110*, 724.
(44) Ahlrichs, R.; Bär, M.; Häser, M. *Chem. Phys. Lett.* **1989**, *162*, 165.
(45) Häser, M.; Ahlrichs, R. *J. Comput. Chem.* **1989**, *10*, 104.
(46) Zerner, M. C.; Ridley, J. E.; Bacon, A. D.; Edwards, W. D.; Head, J. D.; McKelvey, J.; Culberson, J. C.; Knappe, P.; Cory, M. G.; Weiner, B.; Baker, J. D.; Parkinson, W. A.; Kannis, D.; Yu, J.; Roesch, N.; Kotzian, M.; Tamm, T.; Karelson, M. M.; Zheng, X.; Pearl, G.; Broo, A.; Albert, K.; Li, J.; Hawkins, G. D.; Thompson, J. D.; Kelly, C. P.; Liotard, D. A.; Cramer, C. J.; Truhlar, D. G. ZINDO-MN version 1.2; Quantum Theory Project and University of Minnesota: Gainesville, FL, and Minneapolis, MN, 2005.
(47) Riddick, J. A.; Bunger, W. B. *Organic Solvents*; J. Wiley: New York, 1970.
(48) Cramer, C. J. *Essentials of Computational Chemistry: Theories and Models*, 2nd ed.; John Wiley & Sons: Chichester, U.K., 2004.
(49) Scherer, T.; van Stokkum, I. H. M.; Brouwer, A. M.; Verhoeven, J. W. *J. Phys. Chem.* **1994**, *98*, 10539.
(50) Yoshihara, T.; Druzhinin, S. I.; Zachariasse, K. A. *J. Am. Chem. Soc.* **2004**, *126*, 8535.
(51) Agmon, N. *J. Phys. Chem. A* **2005**, *109*, 13.
(52) Waluk, J.; Komorowski, S. J.; Herbich, J. *J. Phys. Chem.* **1986**, *90*, 3868.
(53) Eilers-König, N.; Kühne, T.; Schwarzer, D.; Vöhringer, P.; Schroeder, J. *Chem. Phys. Lett.* **1996**, *253*, 69.
(54) Grabowski, Z. R.; Rotkiewicz, K.; Rettig, W. *Chem. Rev.* **2003**, *103*, 3899.
(55) Kapelle, S.; Rettig, W.; Lapouyade, R. *Chem. Phys. Lett.* **2001**, *348*, 416.
(56) Gurzadyan, G. G.; Tran-Thi, T.-H.; Gustavsson, T. *J. Chem. Phys.* **1998**, *108*, 385.
(57) Elsaesser, T.; Kaiser, W. *Annu. Rev. Phys. Chem.* **1991**, *42*, 83.
(58) Kovalenko, S. A.; Schanz, R.; Hennig, H.; Ernsting, N. P. *J. Chem. Phys.* **2001**, *115*, 3256.
(59) Horng, M. L.; Gardecki, J. A.; Papazyan, A.; Maroncelli, M. *J. Phys. Chem.* **1995**, *99*, 17311.
(60) Sukowski, U.; Seilmeier, A.; Elsaesser, T.; Fischer, S. F. *J. Chem. Phys.* **1990**, *93*.
(61) Iwata, K.; Hamaguchi, H.-o. *J. Phys. Chem. A* **1997**, *101*, 632.
(62) Benniston, A. C.; Matousek, P.; McCulloch, I. E.; Parker, A. W.; Towrie, M. *J. Phys. Chem. A* **2003**, *107*, 4347.
(63) Pigliucci, A.; Vauthey, E. *Chimia* **2003**, *57*, 200.
(64) Schwarzer, D.; Kutne, P.; Schröder, C.; Troe, J. *J. Chem. Phys.* **2004**, *121*, 1754.
(65) Wintgens, V.; Poulinquen, J.; Kossanyi, J. *Nouv. J. Chim.* **1985**, *9*, 229.
(66) Klessinger, M.; Michl, J. *Excited States and Photochemistry of Organic Molecules*; VCH Publishers: New York, 1995.
(67) *Conical Intersections: Electronic Structure, Dynamics & Spectroscopy*; Domcke, W., Yarkon, D., Köppel, H., Eds.; World Scientific: Singapore, 2004.
(68) Marcus, R. A.; Sutin, N. *Biochim. Biophys. Acta* **1985**, *811*, 265.
(69) Amatatsu, Y. *J. Phys. Chem. A* **2005**, *109*, 7225 and references therein.